

INFLUENCE OF $C_{12}A_7$ ADMIXTURE ON SETTING PROPERTIES OF FLY ASH GEOPOLYMER

PAVEL ROVNANÍK

*Institute of Chemistry, Faculty of Civil Engineering,
Brno University of Technology, Žitkova 17, Brno, Czech Republic*

E-mail: rovnanik.p@fce.vutbr.cz

Submitted August 27, 2010; accepted November 3, 2010

Keywords: Fly ash, Alkali activation, Setting accelerator, Mayenite

Geopolymer material based on coal fly ash from the high temperature combustion activated with alkali silicate is a very cheap and suitable material for temporary and non-load-bearing structures. For the purposes of emergency application, such as closing barriers, it is necessary to have dry mixtures ready for mixing with water. However, the utilization of dried sodium silicate activator instead of an aqueous solution considerably delays its setting. The application of $C_{12}A_7$ accelerates the setting of alkali activated fly ash, but it also influences its mechanical properties. Early-age strengths are increased, the long term strengths are, however, deteriorated in comparison with the pure material without $C_{12}A_7$. Microstructural changes are described by means of mercury intrusion porosimetry, SEM, XRD and FTIR analysis.

INTRODUCTION

Fly ash is a waste material produced by a high temperature combustion of coal. It can be considered a pozzolanic material because it contains amorphous reactive forms of silicon oxide and aluminosilicates. Therefore, it can be easily activated by alkali hydroxide, silicate or carbonate solutions and sets to form a hardened geopolymeric structure [1-4]. Alkali activated fly ash materials seem to be a good and cheap alternative for materials used for the building of temporary monolithic blocks, e.g. explosion resistant closures of mining works or an immobilization of heavy metals and radioactive waste materials. The aim of this work is to prepare a quick-setting solid material ready to use when mixed with water for the construction of closing barriers in rooms with a sudden risk of fire or explosion occurrence or for the fast immobilization of toxic waste materials. Such material should satisfy several technological demands among which the most important are the quick setting and strength development, easy handling, liquid consistency for a possible pipeline transportation, and it should be environmentally friendly [5].

Alkali activation of aluminosilicates is usually performed by an aqueous solution of alkali hydroxide, silicate or carbonate. However, for the application in hazardous conditions it is necessary to produce "ready-to-use" mixture containing the solid activator that is

readily dissolved when mixed with water and that would set within a short time. Since the utilization of a water glass solution had been well experienced in the previous research [6] it was obvious to apply a solid sodium silicate as an activator. Unfortunately, it brings along some disadvantages among which the most problematic is a delayed setting. One way how to shorten the setting time is curing at an elevated temperature which is quite complicated to provide just at the place of casting. The other possibility is the addition of mineral accelerators to the primary mixture. Ordinary setting accelerators used for OPC concrete are based on alkali salts such as silicates, carbonates and aluminates. Since soluble silicates and carbonates are generally used as alkali activators, only quick-setting aluminates would probably be the effective accelerators in case of fly ash geopolymers.

A $C_{12}A_7$ -based accelerator used in this study can set and harden in 1 to 3 minutes using a reaction with water and has the quickest hydration reaction of all calcium aluminate minerals. Crystalline $C_{12}A_7$ produces mainly C_2AH_8 in the case of sole hydration, and then it is slowly transformed to C_3AH_6 [7]. Amorphous $C_{12}A_7$ is the best quick-setting agent known and can result in a mixture of C_2AH_8 and C_4AH_x ($x = 13$ or 19) during hydration. When mixed with Portland cement it reacts with $Ca(OH)_2$ and $CaSO_4$ to form acicular $C_3A \cdot 3CaSO_4 \cdot 32H_2O$ (ettringite) crystals with a high initial strength [8].

This work evaluated an effectiveness of the $C_{12}A_7$ -based accelerator on the shortening of setting time of fly ash based geopolymer mixtures and how this admixture affects the mechanical properties and microstructure of the hardened geopolymer. The results were compared with those obtained for geopolymer mixtures without setting accelerator.

EXPERIMENTAL

The basic geopolymer was prepared from fly ash and dried sodium silicate. Fly ash was obtained from a high temperature combustion of black coal. It was provided by a thermal power plant in Dětmarovice (ČEZ, a. s.) and its chemical composition was (wt.%): SiO_2 49.82, Al_2O_3 24.67, Fe_2O_3 7.05, CaO 3.91, MgO 2.68, S_{total} 0.91, Na_2O 0.70, K_2O 2.78. Dried sodium silicate was purchased from Henkel AG under the brand name Portil A. The chemical composition of sodium silicate was (wt.%): SiO_2 50.75, Na_2O 26.78, H_2O 22.47 with a silicate modulus (SiO_2/Na_2O) equal to 1.95. Calcium aluminate $C_{12}A_7$ (mayenite) was prepared by a solid-state reaction of limestone and alumina (Alcan). Powdered limestone and alumina were mixed in a molar ratio $CaCO_3/Al_2O_3 = 12 : 7$, consolidated with a small amount of water and extruded. Prepared granules were heated in an electrical furnace at $1325^\circ C$ for 1 h. The heating rate was set to $4^\circ C/min$. Prepared mayenite was let cool down on the air and ground. Its fineness was measured by means of a laser granulometry on Mastersizer Hydro 2000 MU (A) equipment in a liquid ethanol. The average grain size of mayenite is $d_{50} = 12.6$ μm and $d_{90} = 59.9$ μm . The purity of mayenite was checked by an XRD analysis that revealed small amount of spinel as the main impurity originating from alumina.

Nine sets of specimens were prepared by mechanically mixing of fly ash with alkali activator, $C_{12}A_7$ powder and water. At first, a dry mixture of fly ash, Portil A and accelerator was homogenized and then a sufficient

amount of water was added to prepare a slurry. Three specimens were prepared without the addition of the accelerator and they were considered reference samples. The composition of the mixtures is listed in Table 1. The mixtures are labeled according to the percentage of Portil A and calcium aluminate with respect to the amount of fly ash. The slurry was cast into prismatic moulds with dimensions $20 \times 20 \times 100$ mm and vibrated for 1 min to remove the entrained air. Prepared specimens were stored at $20^\circ C$ and an ambient humidity until tested.

The hardened pastes were tested for their mechanical properties at the age of 24 hours and 28 days. Flexural strengths were determined using a standard three-point-bending test and compressive strengths were measured on far edge of both residual pieces obtained from the flexural test according to EN 196-1 standard. Setting time was evaluated using Vicat equipment in accordance with the standard procedure described in EN 196-3.

A pore distribution was evaluated by means of a mercury intrusion porosimetry (MIP) analysis that was conducted on paste samples using Micromeritics Poresizer 9300 porosimeter that can generate a maximum pressure of 207 MPa and evaluate a theoretical pore diameter of 0.006 μm . The MIP test is performed in two steps: the low pressure step first evacuates gases, fills the sample holder with mercury and performs porosimetry from about 7 to 179 kPa; the high pressure step reaches pressures between 414 kPa and 207 MPa. The contact angle and surface tension assumed for all tests were 130° and 485 dyn/cm, respectively. FTIR spectra of the finely ground samples were taken using Nicolet 380 FTIR spectrometer, with a single reflectance silicon ATR attachment. The FTIR spectra were collected in the absorbance mode from 400 to 4000 cm^{-1} at resolution of 2 cm^{-1} and 128 scans per spectrum. X-ray diffraction analyses were carried out using Bruker D8 Advance system equipped with Cu tube ($\lambda_{K\alpha} = 1.54184\text{ \AA}$). The evaluation of X-ray scans was done using Diffrac software. Micrographs of alkali activated fly ash pastes were taken on scanning electron microscope Tescan VEGA II XMU. The experiments were carried out on dry samples that were spluttered with copper.

Table 1. Composition of the mixtures.

Component	Fly ash (g)	Portil A (g)	$C_{12}A_7$ (g)	Water (ml)
P15	300	45	-	134
P20	300	60	-	136
P25	300	75	-	138
P15C10	300	45	30	162
P15C15	300	45	45	165
P15C20	300	45	60	171
P20C10	300	60	30	162
P20C15	300	60	45	165
P20C20	300	60	60	171
P25C10	300	75	30	162
P25C15	300	75	45	165
P25C20	300	75	60	171

RESULTS AND DISCUSSIONS

A setting time is a limiting factor for the application of fly ash geopolymer in hazardous conditions. Pure fly ash based geopolymer began to set at the age of 3-9 h depending on the composition but the end of setting was delayed to approximately 24 h after mixing in the case of mixtures P20 and P25. For this reason a $C_{12}A_7$ -based mineral admixture was applied to reduce the setting time. Although sodium silicate has a slightly retarding effect on the hydration of calcium aluminate cements [9], the application of such an accelerator considerably decreased the final setting time to the maximum value of

9 h and it could be even reduced to approx. 6 h with 20 % content of $C_{12}A_7$ (Figure 1). Unfortunately, it still might be quite a long time for the application in hazardous situations with a risk of fire or explosion. It seems to be a bit strange that in the mixture with 15 % of activator the accelerator has a very little effect on the setting time of the material. There is also an adverse trend in the setting time as a function of the accelerator content. For non-accelerated mixture the setting time was prolonged with a higher content of Portil A whereas for the mixtures with $C_{12}A_7$ the setting time decreased. This great paradox is also in contrast with other research studies, where a decrease in setting time for the pure fly ash geopolymer with a higher dosage of alkali activator was observed [10].

The compressive and flexural strengths of tested materials are presented in Figures 2 and 3. The compressive strengths of accelerated specimens at the age of 28 days are bit lower by 5 to 10 MPa compared to reference specimens without $C_{12}A_7$, yet they do not drop under 5 MPa, which is the minimum value required for closing barriers [5]. However, more favourable values were observed for early-age strengths ranging from 2.4 to 7 MPa, while compressive strength at the age of 24 hours could not have been measured for reference mixtures without accelerator due to their very weak structure.

If we compare compressive strengths with corresponding flexural strengths (Figure 3), it is obvious that all trends that can be found in the comparison of the flexural strengths resemble those observed for the compressive strengths. The values of early-age strengths exceed 1 MPa, except for the accelerated mixtures containing only 15 % of activator and, of course, also the reference mixtures without $C_{12}A_7$. The standard values of flexural strength measured at the age of 28 days range between 2 and 4.5 MPa, which is sufficient for many application purposes. However, the least progress in strength's development was surprisingly observed for specimens with 25 wt.% activator and 20 wt.% $C_{12}A_7$ (P25C20),

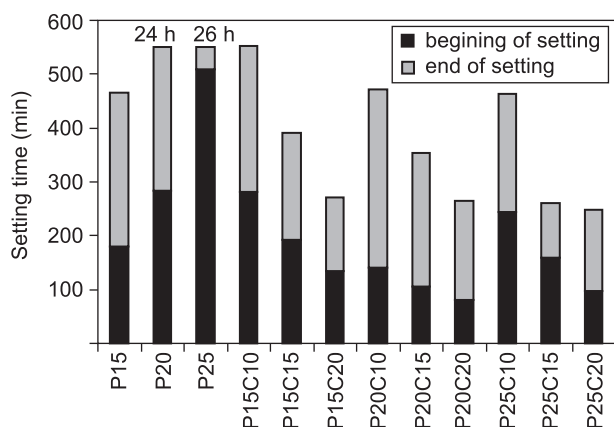


Figure 1. Setting times of fly ash based geopolymer mixtures. Final setting times of the mixtures P20 and P25 are not depicted because they reached 24 h and 26 h, respectively.

where the difference between 24 h and 28 days strength is only 0.1 MPa. This is in a great contrast with 80 % increase of the corresponding compressive strength.

Investigation of a pore structure of the fly ash geopolymer was carried out by means of mercury intrusion porosimetry. Differences in the pore distribution of tested mixtures are presented in Figure 4. The Figure 4a compares the pore distribution of geopolymer without the setting accelerator and with respect to various dosage of alkali activator. The maximum pore volume appears to be in the range of large capillary pores between 1 and 10 μm for all three mixtures. The cumulative pore volume slightly decreases with an increasing amount of activator in the sample and these findings perfectly correlate with compressive strengths at the age of 28 days because the values of strength are reciprocally proportional to the volume of capillary pores. If mayenite as a setting accelerator is added to the mixture, the size of large capillary pores decreases and mainly smaller capillary pores predominate in the structure of the geopolymer paste. The effect of mayenite dosage is not so significant but it seems that the material tends to form slightly smaller pores with a decreasing amount of mayenite. Porosity of samples with $C_{12}A_7$ is generally decreased in comparison

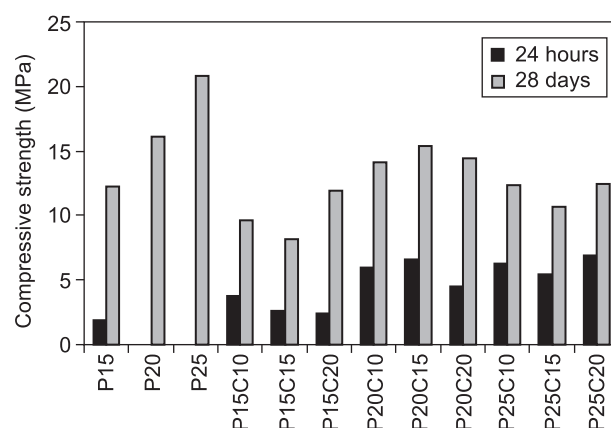


Figure 2. Compressive strengths of fly ash based geopolymers.

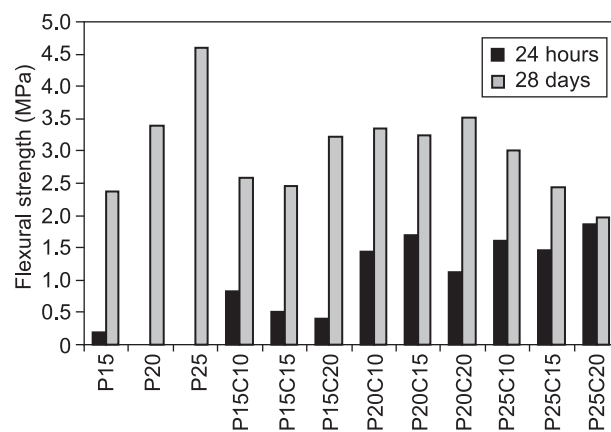


Figure 3. Flexural strengths of fly ash based geopolymers.

with the original fly ash geopolymer but in the case of mixtures with the highest amount of alkali activator the cumulative intruded volume of accelerated mixtures is slightly increased. This difference is, however, caused rather by the reduction in the number of gel and small capillary pores in the matrix of a P25 mixture than by a relatively denser structure.

The SEM micrographs of fracture surfaces of a pure geopolymer matrix and a geopolymer with the addition of $C_{12}A_7$ accelerator are shown in Figure 5. The first micrograph revealed plenty of unreacted fly ash spheres sparsely connected via the amorphous geopolymeric binder. Such poorly reacted matter can be attributed to the utilization of a solid alkali activator and its relatively high silicate modulus. The corresponding concentration of alkalis varies in the series of mixtures with 15, 20 and 25 % alkali activator from 2.7 to 4.2 M NaOH. This concentration is relatively low for the sufficient dissolving ability of fly ash particulates to produce reactive monomers that would result in the formation of geopolymeric gel [11]. When a $C_{12}A_7$ -based accelerator is added to the starting mixture it rapidly reacts with water and reactive silicate species to form calcium aluminate or aluminosilicate hydrates. Since $C_{12}A_7$ increases a pH of the alkali solution it also enhances the dissolution of

reactive fly ash particulates and thus contributes to the enhanced formation of geopolymer gel. This mainly amorphous matter is clearly visible in Figure 5b.

XRD curves of original fly ash and fly ash geopolymer pastes are shown in Figure 6. The patterns reveal occurrence of just two dominant crystalline phases which were assigned to quartz and mullite. Lines of these minerals can be observed in all curves, hence it means that these crystalline phases were not produced during hardening process and they originate in fly ash itself. Other minor crystalline phases were detected only in the geopolymer with $C_{12}A_7$ admixture. Some minor XRD peaks indicated unreacted mayenite ($C_{12}A_7$) together with spinel which comes from $C_{12}A_7$ as an impurity. Occurrence of a limited amount of calcite in this sample may be explained by a partial carbonation of calcium rich amorphous phase originated from $C_{12}A_7$. Since the geopolymer matter is known to be amorphous it is generally represented by diffuse peak centered at approximately $27\text{--}29^\circ 2\theta$ [3, 12] which is slightly shifted to higher angles in comparison with amorphous silica peak in fly ash pattern (Figure 6).

Infrared spectra were recorded for the original fly ash and samples of geopolymer without admixture (P20) and with 15 % $C_{12}A_7$ (P20C15) in order to show the effect of

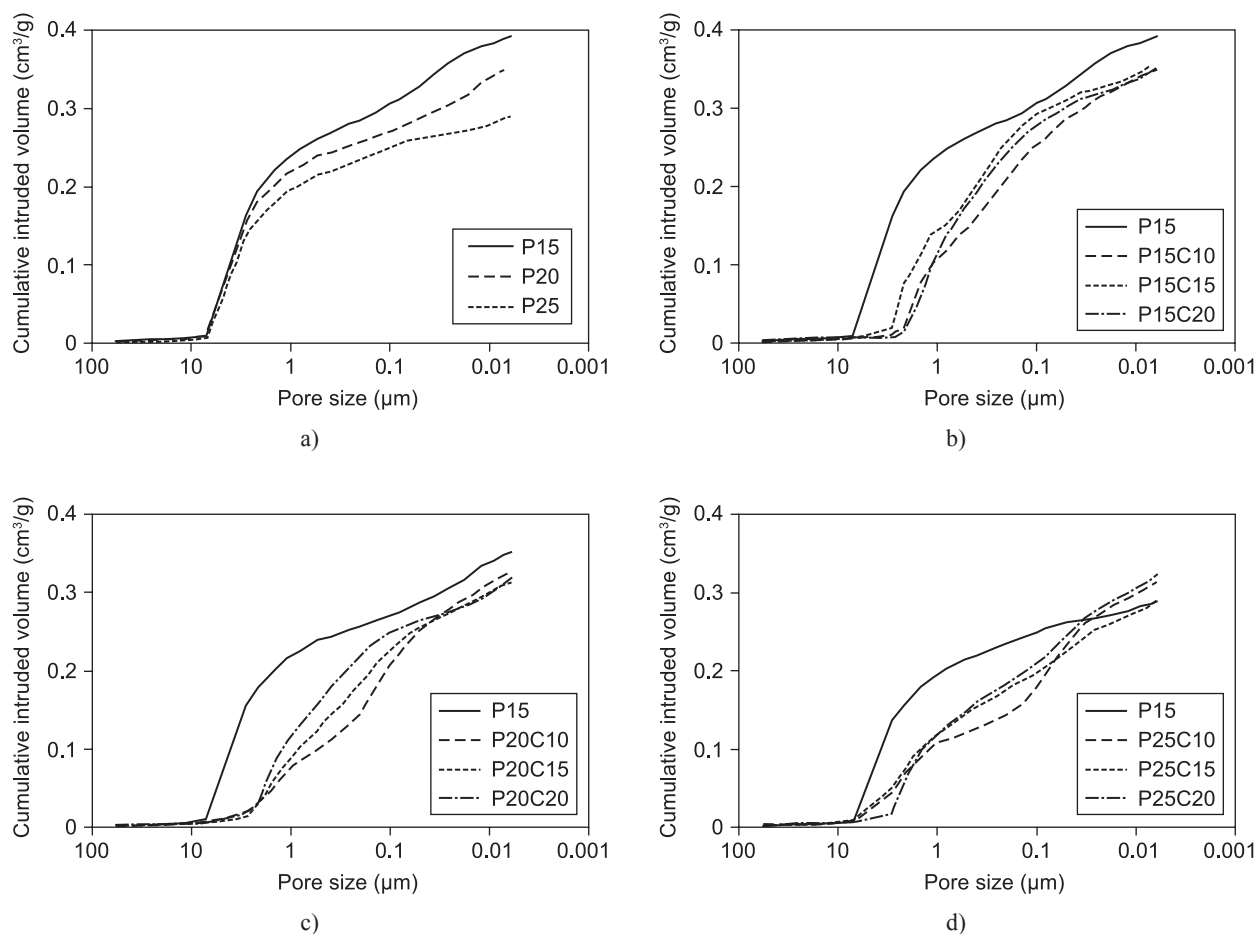


Figure 4. Comparison of pore distribution of geopolymer materials: (a) influence of activator dosage, (b-d) influence of setting accelerator dosage.

aluminate admixture on changes in microstructure. The corresponding infrared spectra are displayed in Figure 7 showing the most important region of spectra between 400-1600 cm^{-1} with features concerning aluminosilicate network. The main broad band at $\sim 1000 \text{ cm}^{-1}$ is assigned to asymmetric stretching vibrations of Al–O and Si–O bonds originating from individual tetrahedra TO_4 [13,14]. The second most intensive band at $\sim 450 \text{ cm}^{-1}$ which is typical for geopolymers has been attributed to the in-plane bending modes of Al–O and Si–O linkages [15, 16]. There was also found a broad band with relatively low intensity centered at $\sim 3300 \text{ cm}^{-1}$ and a small band at 1652 cm^{-1} due to stretching and bending vibrations of H_2O which are not displayed. These bands have been

observed only for geopolymerized fly ash samples and they indicate a presence of hydrated species. The two large bands at 1457 and 1420 cm^{-1} has been reported to be due to the carbonation of soluble alkali species [17]. The ν_3 -carbonate band centered near 1420 cm^{-1} indicates calcite polymorph of calcium carbonate whereas the band at higher frequency belongs to another form of carbonate specie [18]. Shoulders at 1160 and 1084 , double band at 793 and 778 , and the bands at 621 , 514 , and 459 cm^{-1} , which can be observed in IR spectra of the fly ash and sample P20 are assigned to quartz as the crystalline phase in the original fly ash [13], whereas the bands at 1116 , 950 , 730 , 599 , 548 and 501 cm^{-1} have been attributed to mullite crystals [19].

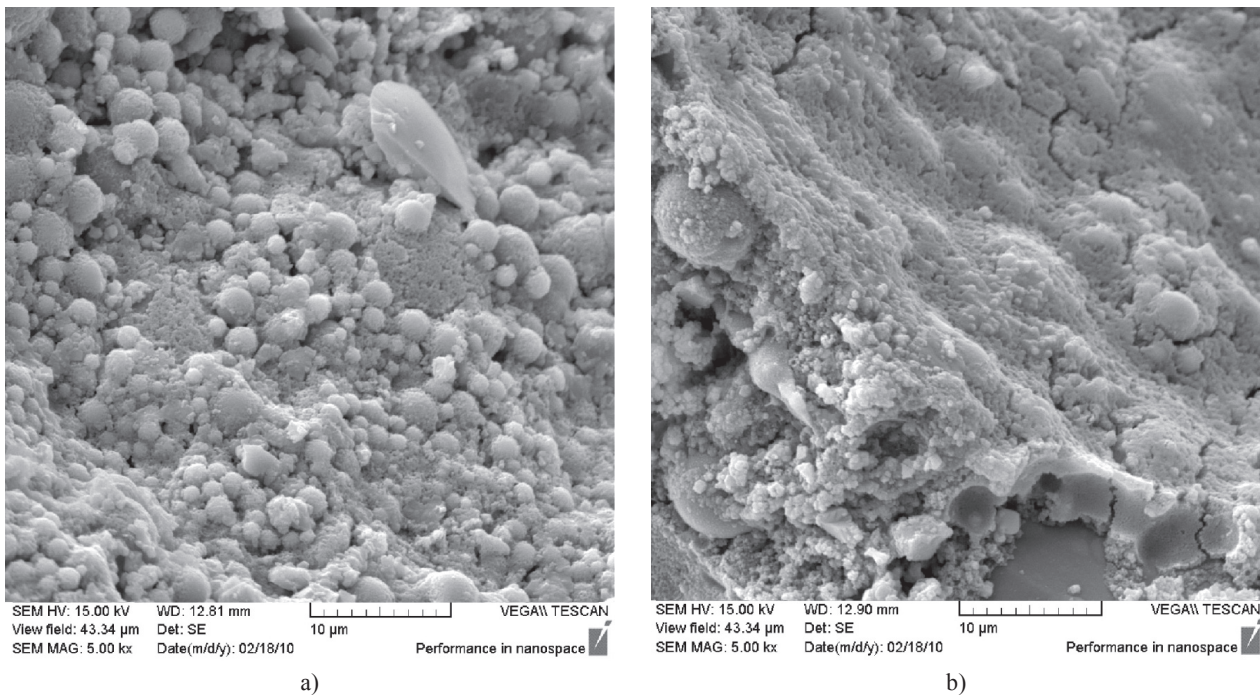


Figure 5. SEM micrographs of geopolymer pastes: a) P20 - without C_{12}A_7 , b) P20C15 - with C_{12}A_7 .

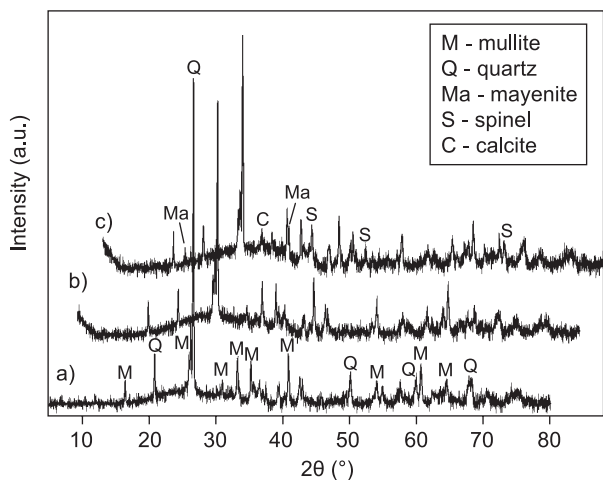


Figure 6. XRD curves of geopolymer pastes: a) unreacted fly ash, b) P20 - without C_{12}A_7 , c) P20C15 - with C_{12}A_7 .

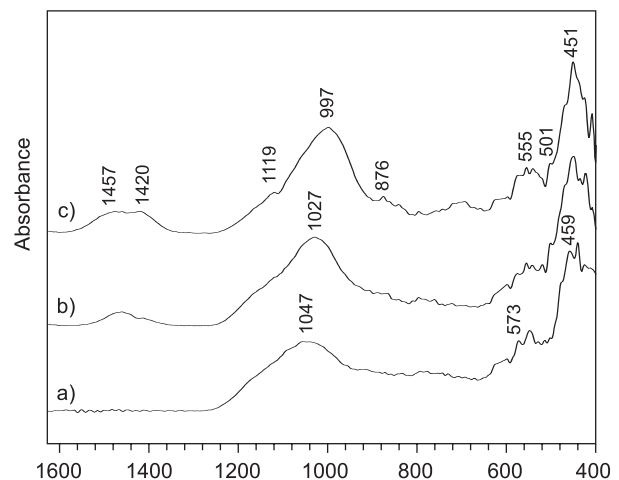


Figure 7. FTIR spectra of geopolymer pastes: a) unreacted fly ash, b) P20 - without C_{12}A_7 , c) P20C15 - with C_{12}A_7 .

The main difference between the spectra of fly ash and both alkali activated pastes is in the position of the broad band in the region $900\text{--}1250\text{ cm}^{-1}$ which shifts from 1047 to 997 cm^{-1} . This band is actually an overlap that results from the superposition of Al–O and Si–O stretching modes of both crystalline and vitreous phases. Shift of this feature to lower frequencies is connected with the geopolymerization reaction of a vitreous phase in the original ash [14, 20]. Such shift occurs as a consequence of weaker Al–O bonds when silicon in TO_4 network is substituted by aluminum and/or due to presence of more depolymerized SiO_4 units [21]. Thus, a significant decrease in frequency of T–O–T stretching vibrations for the material with $C_{12}A_7$ admixture in comparison with the pure geopolymer reveals that some aluminum from $C_{12}A_7$ is incorporated in the tetrahedral network of amorphous geopolymer gel. The low frequency region $500\text{--}900\text{ cm}^{-1}$ is very difficult to interpret. Since the structure of geopolymer gel is mainly amorphous the bands associated with hexacoordinated aluminum and pseudolattice vibrations are diffused and they form a large overlap in which only some minor features can be observed. A weak feature at 876 cm^{-1} in the spectrum of sample with mayenite admixture may be assigned to Al–OH bending vibration of AlO_6 units in calcium aluminate hydrates that arise from partial hydration of $C_{12}A_7$ [22].

CONCLUSIONS

The effect of a calcium aluminate $C_{12}A_7$ cement on the mechanical properties and microstructure of fly ash geopolymer has been investigated. Experimental results show that the addition of calcium aluminate admixture considerably reduces the setting time of fly ash geopolymer by as much as 20 h with respect to the composition. However, the minimum setting time of 6 h might still not be satisfactory for some practical purposes. On the other hand, the addition of $C_{12}A_7$ into geopolymer mixture causes a decrease in both 28-days flexural and compressive strengths in comparison with the reference geopolymer. This observation becomes marked especially with an increasing content of activator, but the absolute values do not drop under 5 MPa for the compressive strength and 2 MPa for the flexural strength.

XRD, SEM, FTIR and MIP techniques were employed to characterize the microstructure of hardened matter and to show the differences between pure fly ash geopolymer and geopolymer with the addition of calcium aluminate admixture. The microstructure analysis shows that $C_{12}A_7$ is involved in the main geopolymerization process as there were observed no new crystalline phases in the matrix that could be assigned to the formation of separate hydrated calcium aluminate species. These findings were also confirmed by the FTIR analysis

revealing that the tetrahedral SiO_4 and AlO_4 network of a vitreous phase in the samples with $C_{12}A_7$ is enriched with Al.

Acknowledgements

This paper was elaborated with the financial support of the projects granted by the Czech Science Foundation (grant no. GP103/08/P270) and the Ministry of Education, Youth and Sports of the Czech Republic (grant no. MSM 0021630511). The author wishes to gratefully acknowledge Dr Patrik Bayer for carrying out porosimetry measurements.

References

- Palomo, A., Grutzeck, M.W., Blanco, M.T.: *Cem. Concr. Res.* 29, 1323 (1999).
- Katz, A.: *Cem. Concr. Res.* 28, 197 (1998).
- Duxson, P., Fernández-Jiménez, A., Provis, J.L., Lucey, G.C., Palomo, A., Van Deventer, J.S.J.: *J. Mater. Sci.* 42, 2917 (2007).
- Shi, C., Krivenko, P.V., Roy, D.: *Alkali-Activated Cements and Concretes*, p. 277-286, Taylor&Francis, Londo
- Lukš, J., Lebedová, Z. in: *Proceedings of the 13th International Seminary: Reinforcement, sealing and anchoring of rock massive and building structures 2008*, p. 193-196, Ed. Aldorf, J., Janiček, D., VŠB-TU, Ostrava 2008. (in Czech)
- Rovnaník, P. in: *Non-Traditional Cement and Concrete III*, p. 662-667, Brno University of Technology, Brno 2008.
- Park, C.K.: *Cem. Concr. Res.* 28, 1357 (1998).
- Park, H.G., Sung, S.K., Park, C.G., Won, J.P.: *Cem. Concr. Res.* 38, 379 (2008).
- Ding, J., Fu, Y., Beaudoin, J.J.: *Cem. Concr. Res.* 26, 799 (1996).
- De Silva, P., Sagoe-Crentsil, K., Sirivivatnanon, V.: *Cem. Concr. Res.* 37, 512 (2007).
- Wang, H., Li, H., Yan, F.: *Colloids and Surfaces A: Physicochem. Eng. Aspects* 268, 1 (2005).
- Rattanasak, U., Chindaprasirt, P.: *Miner. Eng.* 22, 1073 (2009).
- Fernández-Jiménez, A., Palomo, A.: *Microporous and Mesoporous Mater.* 86, 207 (2005).
- Criado, M., Fernández-Jiménez, A., Palomo, A.: *Microporous and Mesoporous Mater.* 106, 180 (2007).
- Phair, J.W., Van Deventer, J.S.J.: *Int. J. Miner. Process.* 66, 121 (2002).
- Dimas, D., Giannopoulou, I., Panias, D.: *J. Mater. Sci.* 44, 3719 (2009).
- Yousuf, M., Mollah, A., Hess, T.R., Tsai, Y.-N., Cocke, D.L.: *Cem. Concr. Res.* 23, 773 (1993).
- Fernández-Carrasco, L., Ruis, J., Miravittles, C.: *Cem. Concr. Res.* 38, 1033 (2008).
- Voll, D., Lengauer, C., Beran, A., Schneider, H.: *Eur. J. Mineral.* 13, 591 (2001).
- Rovnaník, P.: *Constr. Build. Mater.* 24, 1176 (2010).
- Clayden, N.J., Esposito, S., Aronne, A., Pernice, P.: *J. Non-Cryst. Solids* 258, 11 (1999).
- Fernández-Carrasco, L., Vázquez, E.: *Fuel* 88, 1533 (2009).